ARTICLE IN PRESS

Brain Stimulation xxx (2015) 1–8

Contents lists available at ScienceDirect

Brain Stimulation

journal homepage: www.brainstimjrnl.com

Original Research

Neurochemical Modulation in Posteromedial Default-mode Network Cortex Induced by Transcranial Magnetic Stimulation

Dídac Vidal-Piñeiro [a], Pablo Martín-Trias [a], Carles Falcón [b], Núria Bargalló [c,d], Imma C. Clemente [e], Josep Valls-Solé [f], Carme Junqué [a,c], Alvaro Pascual-Leone [g,h], David Bartrés-Faz [a,c,*]

[a] Department of Psychiatry and Clinical Psychobiology, Faculty of Medicine, University of Barcelona, Spain
[b] Medical Imaging Group, University of Barcelona, CIBER-BBN, Spain
[c] Institut d'Investigacions Biomèdiques August Pi i Sunyer (IDIBAPS), Spain
[d] Neuroradiology Section, Radiology Service, Centre de Diagnòstic per la Imatge, Hospital Clinic de Barcelona, Spain
[e] Department of Psychiatry and Clinical Psychobiology, Faculty of Psychology, University of Barcelona, Spain
[f] EMG Unit, Neurology Service, Hospital Clínic de Barcelona, Barcelona, Spain
[g] Berenson-Allen Center for Noninvasive Brain Stimulation, Beth Israel Deaconess Medical Center, Harvard Medical School, Boston, MA, USA
[h] Institut Universitari de Neurorehabilitació Guttmann, Universitat Autònoma de Barcelona, Badalona, Spain

ARTICLE INFO

Article history:
Received 21 November 2014
Received in revised form
8 April 2015
Accepted 10 April 2015
Available online xxx

Keywords:
Transcranial magnetic stimulation
Default-mode network
GABA
Magnetic resonance spectroscopy
fMRI connectivity
Plasticity

ABSTRACT

Background: The Default Mode Network (DMN) is severely compromised in several psychiatric and neurodegenerative disorders where plasticity alterations are observed. Glutamate and GABA are the major excitatory and inhibitory brain neurotransmitters respectively and are strongly related to plasticity responses and large-scale network expression.
Objective: To investigate whether regional Glx (Glutamate + Glutamine) and GABA could be modulated within the DMN after experimentally-controlled induction of plasticity and to study the effect of intrinsic connectivity over brain responses to stimulation.
Methods: We applied individually-guided neuronavigated Theta Burst Stimulation (TBS) to the left inferior parietal lobe (IPL) in-between two magnetic resonance spectroscopy (MRS) acquisitions to 36 young subjects. A resting-state fMRI sequence was also acquired before stimulation.
Results: After intermittent TBS, distal GABA increases in posteromedial DMN areas were observed. Instead, no significant changes were detected locally, in left IPL areas. Neurotransmitter modulation in posteromedial areas was related to baseline fMRI connectivity between this region and the TBS-targeted area.
Conclusions: The prediction of neurotransmitter modulation by connectivity highlights the relevance of connectivity patterns to understand brain responses to plasticity-inducing protocols. The ability to modulate GABA in a key core of the DMN by means of TBS may open new avenues to evaluate plasticity mechanisms in a key area for major neurodegenerative and psychiatric conditions.

Introduction

In the last two decades, resting-state fMRI (rs-fMRI) studies have identified the presence of certain components that fluctuate synchronously [1,2], which are thought to reflect the intrinsic functional architecture of the brain. One of the resting-state networks (RSN), the default-mode network (DMN), has been intensively investigated [3]. This network is comprised of posteromedial structures (precuneus/posterior cingulate cortex [PCC]), medial prefrontal cortex (mPFC), lateral inferior parietal lobes (IPL) and temporal nodes. The DMN shows high activity at rest, while its nodes exhibit decreased engagement during externally oriented tasks [4]. This network is compromised in several neuropsychiatric

Abbreviations: DMN, Default-mode network; GM, Grey Matter; IPL, Inferior parietal lobe; hr, High-resolution; MRS, Magnetic resonance spectroscopy; mPFC, Medial prefrontal cortex; mr, Medium-resolution; PCC, PosteriorCingulate/Precuneus; ROI, Region-of-interest; rs-fMRI, Resting-state functional magnetic resonance spectroscopy; RSN, Resting-state network; NIBS, Non-invasive brain stimulation; (i/c)TBS, (intermittent/continuous) Theta-burst stimulation; (r)TMS, (repetitive) Transcranial magnetic stimulation; tCr, Total Creatine; tNAA, Total N-Acetylaspartate; VOI, Voxel-of-interest; WM, White Matter.

This work was supported by a research grant from the Spanish Ministerio de Economia y Competitividad (PSI2012-38257) to Dr. David Bartrés-Faz. Dr. Alvaro Pascual-Leone was supported by a grant from the National Institutes of Health – Harvard Clinical and Translational Science Center/Harvard Catalyst (UL1 RR025758).

* Corresponding author. Department of Psychiatry and Clinical Psychobiology Faculty of Medicine, University of Barcelona, Casanova, 143, 08036 Barcelona, Spain. Tel.: +34 934039295; fax: +34 93 4035294.
E-mail address: dbartres@ub.edu (D. Bartrés-Faz).

http://dx.doi.org/10.1016/j.brs.2015.04.005
1935-861X/

disorders, such as schizophrenia [5,6], autism [7], Alzheimer's disease [8,9], and even healthy aging [10]. Alterations in the DMN are often reflected by reductions in connectivity between nodes, reduced resting-state metabolism, and a lack of task-induced deactivation.

Glutamatergic and GABAergic neurons are the main excitatory and inhibitory constituents of the canonical microcircuit respectively [11], and hence mediate neuronal activity. Glutamate and GABA neurotransmitters can be non-invasively quantified in humans by MR spectroscopy (MRS) [12], and have consistently been associated with functional neuroimaging measures [13]. Specifically in the DMN, local GABA concentration has shown to predict task-induced deactivations [14], while glutamate showed an inverse pattern, and hence relates to reduced deactivations [15]. Intrinsic functional connectivity of the DMN is also mediated by GABA and glutamate [16]. Complementarily, MRS neurotransmitter measures in the DMN are sensitive to healthy and pathological aging [17,18].

In accordance with their fundamental role in mechanisms of neuroplasticity, GABA and glutamate imbalances [19,20] have been reported in the abovementioned conditions characterized by DMN dysfunction. For example, in Alzheimer's disease neuroplasticity is altered in association with a glutamate/GABA microcircuit dysfunction, which additionally shows complex interactions with Amyloid-beta deposition [21]. Therefore, the ability to modulate glutamate and GABA within the DMN after the application of plasticity-inducing procedures may offer a unique opportunity to evaluate the preservation of regional plasticity mechanisms in a key network for several diseases. Ultimately, brain plasticity responses in the DMN may also be useful to monitor disease progression or response to treatments.

The use of non-invasive brain stimulation techniques (NIBS), such as repetitive transcranial magnetic stimulation (rTMS), has emerged as an optimal methodological approach in humans to induce and evaluate plasticity mechanisms [22]. Patterned protocols of stimulation such as theta-burst stimulation (TBS) [23], can modulate cortical excitability producing long-term potentiation and long-term depression like phenomena, up to an hour after stimulation cessation. Physiological and pharmacological investigations revealed glutamatergic [24] and GABAergic [25] involvement in TBS-induced plasticity effects. Intermittent TBS (iTBS) tends to enhance cortical excitability, while continuous TBS (cTBS) usually produces inhibitory post-effects [23] both in the underlying stimulated tissue and in distal interconnected areas [26]. However NIBS after-effects are highly dependent on a variety of parameters [27] such as functional brain connectivity that mediates the neural and cognitive response to NIBS [26,28].

rTMS can directly modulate DMN expression [29,30] by targeting an accessible cortical node of this network; the left IPL. So far, it has been shown that stimulating this area modulates connectivity changes between DMN nodes [30,31] and enhances alpha rhythm [32]. In addition, MRS, that allows regional quantification of endogenous metabolites, represents a sensitive technique to capture NIBS after-effects [33–36] such as revealing increased GABA concentration in the motor cortex following cTBS [25]. These neurotransmitter modulations after stimulation have been shown to be functionally relevant, as GABA responsiveness to transcranial direct current stimulation was related to greater motor learning capacity and learning-related decrement of fMRI signal [37]. Furthermore other protocols able to elicit plasticity, such as learning paradigms, produce regional neurotransmitters modulations, essentially GABA changes, of similar magnitude to the ones produced by NIBS [38,39].

To the best of our knowledge, no study has so far addressed whether NIBS is capable to modulate GABA or glutamate measures within the DMN. The main objective of this investigation was to study whether a single TBS session would result in the modulation of neurotransmitter concentration in both local and distal DMN nodes (left IPL and PCC) assessed with MRS. Consequently, we applied individually-guided neuronavigated sham, intermittent or continuous TBS stimulation in-between two MRI acquisitions. A rs-fMRI sequence was also acquired before stimulation. We hypothesized that active rTMS would induce neurotransmitter changes, compared to sham stimulation in both local and distal areas. While this study is exploratory, we expected GABA increases after cTBS as in Stagg and colleagues [25] and a reversed effect after iTBS. We also hypothesized that the magnitude of neurotransmitter changes induced by rTMS in the distal node would be related to the intrinsic functional connectivity.

Methods

Participants

Thirty-six healthy right-handed young subjects (age = 23.50 [2.00]; 8 males), naive to stimulation, were randomly assigned to one of three experimental groups (Sham, iTBS or cTBS). Four subjects (1 male) were discarded from the MRS analysis, due to poor quality data. These subjects were not included in any analysis; data from 2 left IPL spectras were removed due to lipid contamination, and one PCC spectra was removed due to MRS acquisition problems. Final analyses included 30 subjects for the left IPL voxel (10 sham, 10 iTBS, 10 cTBS) and 31 subjects for the PCC spectroscopic voxel (11 sham, 10 iTBS, 10 cTBS). No differences regarding gender, age and education existed between groups (see SI for inferential tests and extended sociodemographic information). None of the participants had any neurological or psychiatric disorder or TMS contraindications [40]. All subjects gave informed consent and the protocol was in accordance with the Declaration of Helsinki and approved by the local ethics committee.

Experimental design

The main experimental protocol consisted of a TMS session in-between two MRI acquisitions. In both MRI sessions, two MRS were acquired, one in the PCC and the other in the left IPL, along with a medium resolution (mr) structural acquisition (Fig. 1). Additionally, in the pre-stimulation session an rs-fMRI dataset was acquired. Prior to the main experimental day, subjects underwent an MRI acquisition that included a high resolution (hr)-3D structural and an rs-fMRI dataset, acquired for segmentation, co-registration and targeting purposes.

TMS

TBS was applied, according to previously described protocols [23], in-between two MRI sessions with a MagPro ×100 Stimulator (MagVenture A|S, Denmark) and an eight-figure coil (TBS and motor threshold protocols are fully described in SI). For the sham group, a sham coil was used mimicking the clicking sound. TMS position was held tangentially to the skull and rotated ≈30–50° from the midline thus being perpendicular to the dorsal part of the anterior occipital sulcus [41]. TBS was performed in a room adjacent to the MRI scanner and was neuronavigated with a stereotactic system (eXimia Navigated Brain Stimulation, Nexstim, Finland).

The stimulation target was individually defined as the coordinates within the left IPL that showed the highest correlation with other DMN nodes. We operationalized this concept in a similar way as described in the literature [29,31]. We created 7 mm spherical Regions-of-Interest (ROI)s in the mPFC (x,y,z = 0,51,−7),

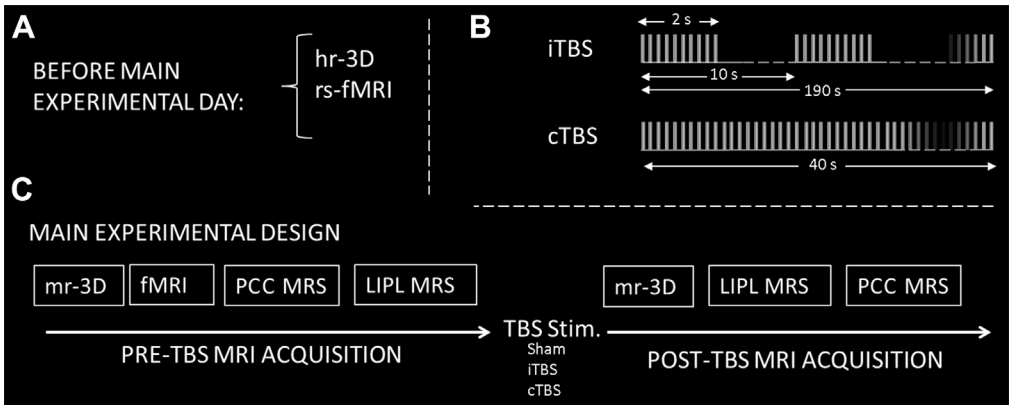

Figure 1. Protocol schema. A) Datasets acquired before the day of the experiment, B) schema of patterned repetitive transcranial magnetic stimulation used in the study and C) timeline schema of the main experimental design.

the PCC (x,y,z = 1,−55,17) and the right IPL (x,y,z = 50,−64,27). This coordinates, published elsewhere [31,42], were transformed to subject's own functional space which was followed by a seed-based connectivity analysis of this ROIs within the left IPL. The targeted point (mean coordinates to MNI: [x,y,x = −45,−67,32]; see Fig. S2 for individual coordinates) was defined as the voxel with maximum conjoint correlation of the abovementioned connectivity maps and stimulation was applied to the nearest scalp point. The connectivity of the target stimulation area was posteriorly studied with the rs-fMRI acquired during the experimental day to evaluate the specificity of this area regarding the DMN during the experimental day (see SI, Fig. S1).

MRI acquisition

All subjects were examined on a 3T MRI scanner (Magnetom Trio Tim, Siemens, Germany). The sequences were acquired with the following parameters:

Structural magnetic resonance images

Three 3D structural datasets were acquired during the experimental design for each subject. One hr-3D sequence (T1-weighted magnetization prepared rapid gradient echo [T1-weighted MPRAGE], sagittal plane acquisition, TR = 2300 ms, TE = 2.98 ms, 240 slices, slice thickness = 1 mm, FOV = 256 mm, matrix size = 256 × 256) was acquired before the main day of the experiment, while two mr-3D datasets were acquired in the pre- and post-stimulation MRI sessions (T1-weighted MPRAGE, sagittal plane acquisition, TR = 1390 ms, TE = 2.86 ms, 144 slices, slice thickness = 0.625 mm, FOV = 240 mm, matrix size = 144 × 384).

Functional MRI (fMRI)

Two 5′ resting-state fMRI datasets (T2*-weighted GE-EPI sequence, TR = 2000 ms, TE = 16 ms, 36 slices per volume, slice thickness = 3 mm, interslice gap = 25%, FOV = 240 mm, matrix size = 128 × 128, 150 volumes) were acquired during the whole experiment, one prior to the main experimental day and the other during the pre-stimulation MRI acquisition.

MRS

Four ^{1}H-MRS spectra were acquired with a MEGA-PRESS sequence during the study; two in the pre-stimulation MRI acquisition and two immediately after TBS stimulation. The spectra were located either in the PCC or the left IPL. MRS was acquired with the following parameters: MEGA-PRESS sequence; 256 spectral averages; TR = 1500 ms; TE = 68 ms; voxel size = 3.0 × 2 × 1.50 cm^3; approximate duration: 10 min. 22 ms double-banded Gaussian pulses were applied at 1.9 or 7.5 ppm in alternate lines to edit the γ-CH_2 resonance of GABA at 3.0 ppm and at 4.7 ppm to suppress water signal ("CHESS" water suppression). The first post-stimulation left IPL and PCC spectral lines were acquired 11 and 20 min after stimulation respectively.

Voxel of interest (VOI) location was guided by structural information as the relatively big area (9 cm^3) of the spectroscopic voxel canceled the advantages of a connectivity-based targeting approach. This methodological limitation has to be taken into account as it might restrict the possibility of placing the spectroscopic voxel in optimum locations. Caudally, the PCC voxel was limited by the parieto-occipital fissure and rostro-inferiorly by the corpus callosum while trying to keep the maximum portion of posterior cingulate cortex. In the left IPL, the VOI was placed below the intraparietal sulcus while trying to encompass to the greatest degree possible the angular gyrus with the angular gyrus and sulcus and the anterior occipital sulcus as key structural references.

Analyses

Neuroimaging analyses were performed with a combination of SPM (segmentation, corregistration; http://www.fil.ion.ucl.ac.uk/spm/), FSL and AFNI (resting-state data; http://fsl.fmrib.ox.ac.uk/fsl/fslwiki/; http://afni.nimh.nih.gov/afni/) softwares. Spectra data were analyzed in frequency domain with LCModel V.6.3-1a [43] (Fig. 2a and b).

Resting-state data preprocessing

Rs-fMRI data preprocessing included removal of the first 5 volumes, motion correction, skull stripping, spatial smoothing (FWHM = 7 mm), grand mean scaling and filtering with both high-pass and low-pass filters (.1 and .01 Hz thresholds). Next, the data were regressed with six rigid body realignment motion parameters, mean white matter (WM) and mean cerebrospinal fluid signal. No global signal regression was used. Registration to an MNI standard space was performed through a two-step linear transformation.

Structural processing

Mr-3D images were co-registered with linear transformations to the previously acquired hr-3D images, which were segmented into tissue type to obtain overlapping and tissue-type composition indices. This latter index was computed as follows: GM/(WM + GM).

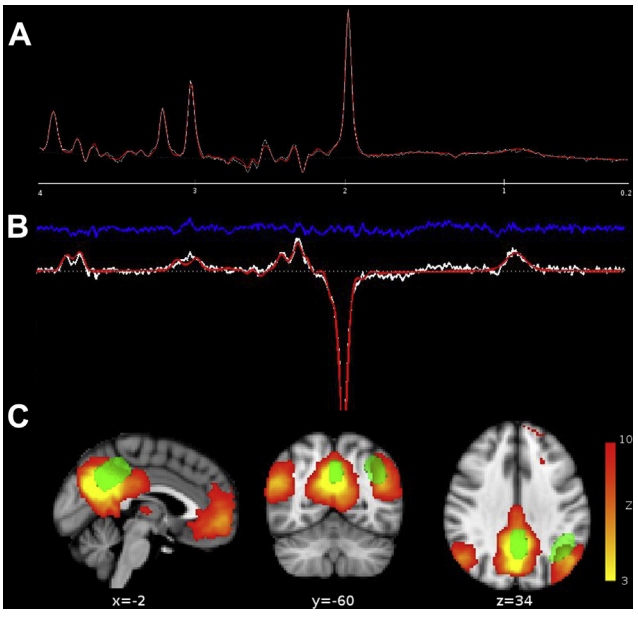

Figure 2. Magnetic Resonance Spectroscopy sequences. A) "Edit OFF" and B) GABA-edited spectra acquired in the left IPL from a representative subject. Grey dotted line represent baseline, the white line the data and the red line represents the fitting. The blue line represents the residuals. C) Mean positioning of PCC and left IPL spectras (thresholded at $n > 20$) in green, overlapping a DMN network published elsewhere [2], arbitrarily thresholded at $z = 3$ in a red-yellow scale. (For interpretation of the references to color in this figure legend, the reader is referred to the web version of this article.)

MRS analyses

For both "edit OFF" and difference spectra, we calculated the best fit of the experimental spectrum as a linear combination of model spectra. Fitting for "edit OFF" was performed over the spectral range from .2 to 4.2 ppm. MEGA-PRESS edited spectra were analyzed using a simulated basis set obtained with density matrix simulation from the sequence using published values for chemical shifts and J-couplings [44]. The fitting was performed between the 1.9–4.0 ppm spectral range. Total creatine (tCR) and total N-acetylaspartate (tNAA) were extracted from the unedited spectra while tNAA, GABA and Glx (Glutamate + Glutamine) measures were extracted from the difference spectra. An scaling factor calculated with the average of tNAA unedited and tNAA from the difference spectra was used to allow the fitted values to be on the same scale [45]. Only Cramér-Rao lower bounds (CRLB) < 15% were considered. The metabolites of interest were expressed as tCR ratios. For simplicity in the text we refer to such ratios as GABA and Glx.

Connectivity analyses

To evaluate the relation between distal neurotransmitter modulation and connectivity, a seed-to-seed connectivity analysis with 6 mm radius spherical ROIs was performed. For each subject, PCC-ROI was created in the center of gravity generated by overlapping pre- and post-TBS spectroscopic VOIs while Stim-ROI was placed in the coordinates used to guide stimulation. After GM masking, rs-fMRI preprocessed ROIs timeseries were extracted and correlated for each subject in the individual functional space.

Data analysis

The main hypothesis which assessed TBS effects on metabolite concentrations (Glx and GABA) was tested using 3 × 2 × 2 repeated measures ANOVA with group (sham × cTBS × iTBS), metabolite (Glx × GABA) and time (pre × post) as independent variables and pre-post difference in tissue-type index as a covariable using SPSS 20.0 software (IL, USA). Two ANOVAs were performed, one for each spectra location (PCC and left IPL). To study the relationship between distal neurotransmitter changes and functional connectivity we performed partial correlations with pre-post difference in tissue-type index as a covariable. Specifically we correlated Glx and GABA changes in the distal node (post-pre TBS ^{1}H-MRS) for each experimental group with Stim-to-PCC rs-fMRI connectivity. Secondary analyses are detailed in the results or in the SI. When not specified, data is presented as mean (SD) and significance is considered at $P < 0.05$.

Results

The descriptive results of neurotransmitter concentration are summarized in Table 1.

In the PCC an interaction of group × time × metabolite was found ($F = 3.776$, $P = 0.036$). Post-hoc testing of simple effects indicated increased GABA concentration after iTBS stimulation compared to Sham and cTBS groups ($F = 1.902$, $P = 0.020$; $F = 2582$; $P = 0.018$; Fig. 3). A main effect of metabolite was found ($F = 1617.188$, $P < 0.001$). Left IPL only showed an expected main effect of metabolite ($F = 1809.782$, $P < 0.001$). No other main effects or interactions were found ($P > 0.1$).

The distal GABA increase after stimulation was positively related to Stim-to-PCC connectivity. In other terms, increments in GABA concentration in the PCC after iTBS were significantly related to pre-TBS functional connectivity between the stimulated area and the posteromedial cortex ($r = .839$, $P = 0.005$; Fig. 4). Additionally, non-significant Glx modulation after iTBS was inversely related to rs-fMRI connectivity ($r = -.729$, $P = 0.026$). Neurochemical modulations in the other experimental groups were unrelated to rs-fMRI connectivity ($P > 0.05$). Post-hoc seed-to-brain analysis showed a good specificity of Stim-to-PCC connectivity measure as a predictor of distal neurotransmitters modulation as only functional connectivity from both Stim-ROI and PCC-ROI with posterior DMN areas – and not with other cortical regions – was related to neurotransmitters modulation in the posteromedial cortex (Fig. S3 and SI for detailed methods and results).

To evaluate the location of spectral VOIs regarding the DMN, a control analysis was performed. Subject-specific voxelwise connectivity maps were obtained by regressing left IPL and PCC ROIs timeseries. After transformation to standard space, individual connectivity maps were compared to reported large-scale RSN [2], and group connectivity maps were obtained by non-parametrical permutation testing. Results showed that PCC VOI was mostly located in the DMN network while left IPL VOI was located in areas of both the left frontoparietal network and the DMN (Fig. S4 and SI for detailed methods and results). No impact of movement with our neuroimaging measures was found (SI).

Table 1
Descriptive MRS-metabolite concentrations.

		MRS descriptives				
		n	pre-TBS GABA	post-TBS GABA	pre-TBS Glx	post-TBS Glx
Left IPL	Sham	10	.039 (.003)	.040 (.004)	.120 (.008)	.116 (.008)
	iTBS	10	.041 (.003)	.040 (.004)	.118 (.009)	.117 (.007)
	cTBS	10	.040 (.005)	.040 (.006)	.108 (.011)	.115 (.011)
	All	30	.040 (.004)	.040 (.005)	.116 (.010)	.116 (.010)
PCC	Sham	11	.043 (.006)	.041 (.007)	.128 (.016)	.129 (.015)
	iTBS	10	.039 (.003)	.043 (.005)	.128 (.006)	.122 (.014)
	cTBS	10	.042 (.006)	.039 (.004)	.116 (.010)	.121 (.012)
	All	31	.042 (.005)	.040 (.006)	.124 (.012)	.125 (.014)

Descriptive MRS-metabolite concentrations for each group. Represented as tCR ratios.

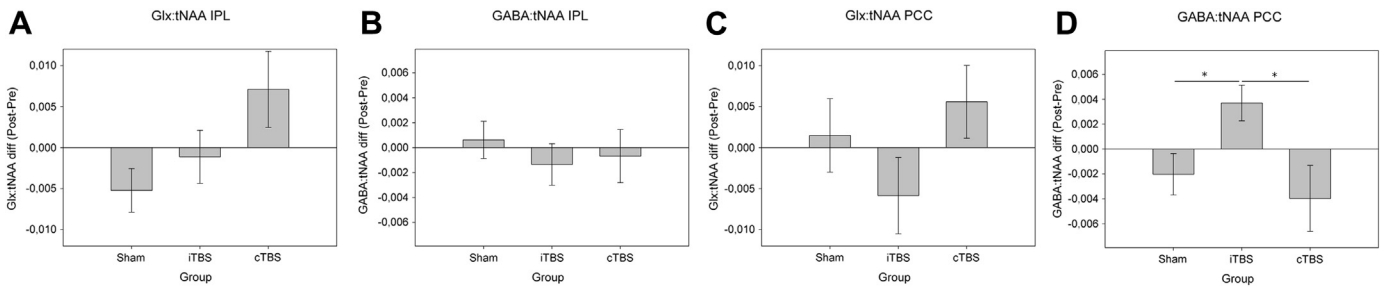

Figure 3. rTMS modulation. rTMS effect in the left IPL over A) Glx and B) GABA. rTMS effect in the PCC over C) Glx and D) GABA. Bars ± SEM represent post-pre changes on metabolite concentrations. Significant modulation of neurotransmitters were observed in the PCU (P= 0.036). Increased GABA after iTBS was found compared to Sham (P = 0.020) and cTBS (P = 0.018) groups.

Discussion

The present study provides the first evidence of regional neurotransmitter modulation within the DMN by means of plasticity-inducing stimulation protocols. The main findings were that iTBS applied to the left IPL increased GABA concentration in the posteromedial cortex and that the magnitude of the induced neurotransmitter modulation in the PCC was significantly associated with the strength of baseline functional connectivity between the TMS-targeted area and this distal region.

Our observation of changes in the metabolite concentrations during an MRS acquisition after the TBS cessation are consistent with current evidence that NIBS techniques can modify regional metabolite concentrations [25,35,36]. After-effects of rTMS on cortical excitability outlast the stimulation period by a few tens of minutes and it is understood as presence of plasticity-like phenomenon [46]. Moreover distal modulation of neurotransmitters is in accordance with established knowledge that shows propagation of TMS effects to distal interconnected areas [47]. Evidences of distal neurotransmitters modulation are in contrast with other studies [33,35]; however the strong functional connectivity at rest between both areas [48] and the great overlapping of resting-state functional and structural connectivity of both areas [49] differ from the previous investigations and it possibly explains the novel observation of distal modulation of metabolites in response to stimulation. Moreover the observation that TBS applied to the IPL modulates the neurochemical characteristics of the posteromedial cortex is not only supported by strong functional connectivity patterns but also, to a great extent, by the presence of direct structural connections. In macaques the multimodal regions of the IPL are richly interconnected to the posteromedial areas, especially the caudal part of the parietal cortex [50–53], that agrees with our targeting location. Neuroimaging studies with humans [54,55] have also found direct structural connectivity between posteriomedial regions and IPL despite known methodological difficulties [56]. Still it is not possible to assess the specificity of distal neurotransmitters modulation regarding the PCC nor to discard that the TBS effects are (partially) driven by indirect pathways. That stands in contrast with

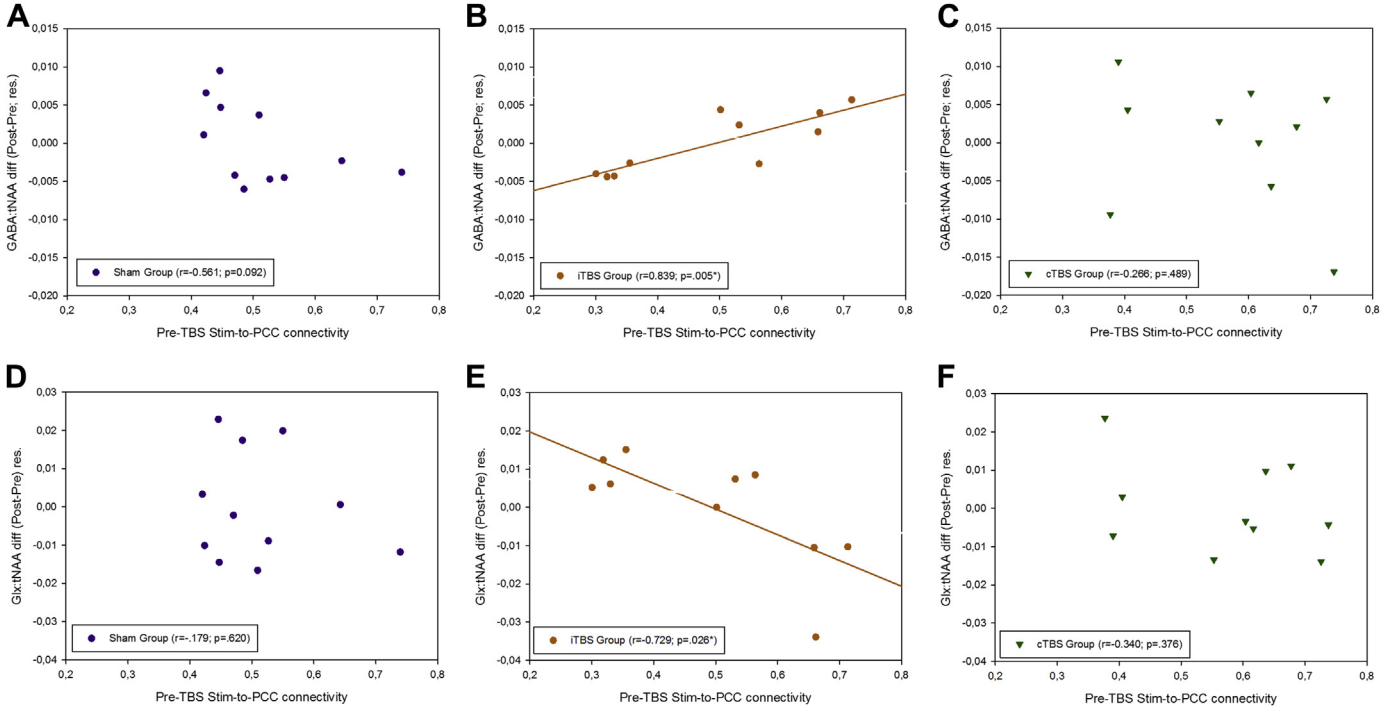

Figure 4. Neurochemical modulation – intrinsic connectivity relationship. Relationship between Stim-to-PCC connectivity and GABA modulation in the PCC after TBS for A) sham B) iTBS and C) cTBS groups. Relationship between Stim-to-PCC connectivity and Glx modulation in the PCC after TBS for D) sham E) iTBS and F) cTBS groups. Values are regressed for post-pre difference in GM/(WM + GM) tissue-type score. Significant relationships between intrinsic connectivity and GABA (P = 0.005) and Glx (P = 0.026) modulation after iTBS was found. See lowe left part of the figure for more stats. Regression line is displayed only for the significant comparisons.

the unfeasibility that neurotransmitter modulation is due to direct effects (local; non-transynaptical) as the depth of the coil is about 2 cm [57]. In the present study we offer novel evidence that distal neurochemical modulation is related to rs-fMRI connectivity between the targeted area and the PCC. These findings add to previous TMS observations indicating that intrinsic functional connectivity is emerging as an effective strategy to guide cortical stimulation to target specific distal areas [29,31]. Relationship of increased baseline connectivity between the TMS target area and the PCC with distal GABA concentration modulation in response to stimulation fits with the interpretation of direct propagation of the effects. Our complimentary analyses further revealed high specificity for the connectivity between the two sites as predictors for this effect, hence reinforcing this interpretation, though a possible contributor effect of voxel placement affecting the relationship could not be rule-out. Altogether the results suggest that connectivity is a variable that it is needed to take into account in further MRS studies.

Our study provides further evidence likely reflecting brain responses to stimulation in order to maintain effective neuronal processing [58], hence revealing putative mechanisms of plasticity as measured by MRS. While it is known that TBS produces changes at different system levels, which needs to be integrated, neurochemical modulation in posteromedial regions can be a specific plastic response of a key node of the DMN. If so, it might have great implications in several neurological or psychiatrical conditions as dysfunction in plasticity mechanisms is common with advancing age [59] and in major neuropsychiatric disorders [19,60], such as Alzheimer's Disease [21,61]. In this regard if it is assumed that GABA responses to TBS reflect cerebral brain plasticity adaptations, our findings may open the possibility of considering MRS-GABA responsiveness as a putative physiological index to interrogate the integrity of plasticity mechanisms in conditions where the posteromedial cortex is particularly compromised, such as initial stages of dementia [62]. Despite further studies are required with samples of patients, studying plasticity mechanisms by NIBS holds promise as a putative physiological marker to monitor the effects of pharmacological and cognitive therapies. Importantly, GABA responsiveness assessed with MRS has already been linked to plasticity responses such as learning mechanisms in the human motor cortex [37,38]. On the other side, *basal* posteriomedial GABA concentrations seems to be decreased in aging [18] and in amnestic mild cognitive impairment [17] as well as it proved sensitive enough to detect pharmacological interventions in the latter condition [63].

While generally iTBS results in prolonged increases of cortical excitability and cTBS leads to the opposite process [23], the complex nature of brain responses to TBS, particularly outside the motor cortex remains to be elucidated. While no directly analogous, our observed direction of spectroscopic changes following stimulation are in contrast with previous literature [25,33–36]. Hence, in the most comparable study, GABA increases in M1 following cTBS were found over this region [25] while we observed a similar result in a distal node after iTBS. We suggest that discrepancies between both findings may be explained by the distinct characteristics of the targeted networks. Neuroimaging techniques point out DMN idiosyncratic properties, such as deactivation during goal-directed external tasks [4], increased metabolism at rest [64], a high correlation between functional and structural connectivity [49], or its emergence in the most stable state of the brain [65]. Intracranial recordings [66,67] further confirmed that DMN has a unique pattern of synaptic activity, which has been postulated as one of the several factors modulating the rTMS brain response [68]. However, it should be noted that discrepancies with previous MRS results can be related to other possibilities instead to idiosyncratic DMN characteristics such as differential cito- and neurotransmitter architectonics [69,70], coil orientation interacting with different gyral morphometry [71] or a differential modulating role of other neurotransmitters [72]. After stimulating left IPL with protocols inducing reduced excitability other studies have found increases in the connectivity and coherence in the DMN [31,32] while after stimulating the IPL with high-frequency TMS reductions of DMN connectivity have been observed. Intra (and inter) network connectivity are known to be modulated by the main inhibitory and excitatory neurotransmitters [13,73], specifically posteromedial Glx:GABA ratio have been linked to DMN expression. This study adds evidence to several papers that found release of dopamine in distal areas after transcranial stimulation by means of Positron Emission Tomography [74,75]. Precisely Cho and Strafella [76] were able to increase dopamine binding in subgenual anterior cingulate cortex after dorsolateral prefrontal cortex stimulation (10-Hz). These two areas belong to two different brain anticorrelated systems [77,78] being the former part of the task-related deactivated (DMN-like) system. While we did not find cTBS modulations of metabolite concentrations we did observed an inverted non-significant pattern compared to iTBS and to the cTBS effect in the motor cortex.

We did not observe significant modulations in Glx after TBS in contrast to some studies that have been able to modulate Glutamate-based MRS measures [33,35,36]. Lack of significant plasticity-induced modulation of regional Glx can be related to the inability to clearly differentiate glutamate from glutamine which plays a role in neural functions and to the involvement of glutamate in several non-synaptic metabolic functions [12]. In summary and according to Stagg [79], our lack of findings regarding Glx may be explained by a limited sensitivity (compared to GABA) of this measure to capture the effects of plasticity though further studies are needed. Similarly we did not found neurochemical modulation in the area underlying stimulation, as hypothesized, but distally in a voxel located in a posteromedial region. Lack of local changes should not be attributed to lack of modulation but to the inability to capture stimulation effects within the DMN. Subsequent analyses confirmed that MRS voxels located in the IPL was significantly contributing to left frontoparietal network as well as to the DMN. While a precise target of the DMN is possible within the IPL area through TMS [29–31], the possibility to place a spectroscopic voxel able to detect MRS changes within the network is more problematic given the size of the spectroscopic voxel and the area of the IPL that contributes to the DMN. In this regard, it is fairly probable that the unique region in the IPL strongly connected, both functionally and structurally, to other DMN areas such as the posteromedial cortex or the parahippocampal cortex, is the posterior part of the angular gyrus also known as PGp in humans and Opt in macaques [51,52,80,81]. The specific location and surface of this area might complicate the placement of a cuboidal VOI able to specifically capture the neurochemicals thus impeding the evaluation of metabolite concentrations within the DMN in this node.

The interpretation of molecular mechanisms accounting for the neurochemical modulation cannot be fully elucidated, as MRS quantifies total neurochemical concentrations and cannot distinguish between different pools [79]. However, GABA-MRS seems to mainly capture tonic extracellular GABA [82]. GABA modulations in our study may be related to upregulation of the glutamic acid decarboxylase enzyme that synthetizes GABA from glutamate [25,35]. Some limitations of our study need to be highlighted. First, some limitations are inherent to the technique and current knowledge on what it assesses [79,83]. Also, the small sample used in our study limits explanatory power and we did not counterbalance the order of left IPL and PCC spectra acquisition. Another limitation refers to the lack of a control voxel outside the DMN thus this study does not allow to evaluate the specificity of neurotransmitters modulation within DMN areas.

In conclusion, this study provides the first evidence that stimulation in the DMN induces dynamic changes in neurotransmitters in distal areas. MRS may provide unique information about plasticity mechanisms outside motor areas. The feasibility of modulating neurotransmitters in the DMN allows the possibility of studying aberrant plasticity in core areas of several neuropsychiatric disorders. Finally, we present the first evidence that neurotransmitter modulation is predicted by connectivity patterns highlighting the relevance of intrinsic patterns of connectivity to understand brain responses to TMS.

Supplementary data

Supplementary data related to this article can be found at http://dx.doi.org/10.1016/j.brs.2015.04.005.

References

[1] Biswal B, Yetkin FZ, Haughton VM, Hyde JS. Functional connectivity in the motor cortex of resting human brain using echo-planar MRI. Magn Reson Med 1995;34:537–41.
[2] Smith SM, Fox PT, Miller KL, et al. Correspondence of the brain's functional architecture during activation and rest. Proc Natl Acad Sci U S A 2009;106:13040–5. http://dx.doi.org/10.1073/pnas.0905267106.
[3] Raichle ME, MacLeod AM, Snyder AZ, Powers WJ, Gusnard DA, Shulman GL. A default mode of brain function. Proc Natl Acad Sci U S A 2001;98:676–82. http://dx.doi.org/10.1073/pnas.98.2.676.
[4] Anticevic A, Cole MW, Murray JD, Corlett PR, Wang X-J, Krystal JH. The role of default network deactivation in cognition and disease. Trends Cogn Sci 2012;16:584–92. http://dx.doi.org/10.1016/j.tics.2012.10.008.
[5] Garrity AG, Pearlson GD, McKiernan K, Lloyd D, Kiehl KA, Calhoun VD. Aberrant "default mode" functional connectivity in schizophrenia. Am J Psychiatry 2007;164:450–7. http://dx.doi.org/10.1176/appi.ajp.164.3.450.
[6] Pujol N, Penadés R, Rametti G, et al. Inferior frontal and insular cortical thinning is related to dysfunctional brain activation/deactivation during working memory task in schizophrenic patients. Psychiatry Res 2013;214:94–101. http://dx.doi.org/10.1016/j.pscychresns.2013.06.008.
[7] Lynch CJ, Uddin LQ, Supekar K, Khouzam A, Phillips J, Menon V. Default mode network in childhood autism: posteromedial cortex heterogeneity and relationship with social deficits. Biol Psychiatry 2013;74:212–9. http://dx.doi.org/10.1016/j.biopsych.2012.12.013.
[8] Greicius MD, Srivastava G, Reiss AL, Menon V. Default-mode network activity distinguishes Alzheimer's disease from healthy aging: evidence from functional MRI. Proc Natl Acad Sci U S A 2004;101:4637–42. http://dx.doi.org/10.1073/pnas.0308627101.
[9] Rombouts SARB, Barkhof F, Goekoop R, Stam CJ, Scheltens P. Altered resting state networks in mild cognitive impairment and mild Alzheimer's disease: an fMRI study. Hum Brain Mapp 2005;26:231–9. http://dx.doi.org/10.1002/hbm.20160.
[10] Andrews-Hanna JR, Snyder AZ, Vincent JL, et al. Disruption of large-scale brain systems in advanced aging. Neuron 2007;56:924–35. http://dx.doi.org/10.1016/j.neuron.2007.10.038.
[11] Logothetis NK. What we can do and what we cannot do with fMRI. Nature 2008;453:869–78. http://dx.doi.org/10.1038/nature06976.
[12] Rae CD. A guide to the metabolic pathways and function of metabolites observed in human brain 1H magnetic resonance spectra. Neurochem Res 2014;39:1–36. http://dx.doi.org/10.1007/s11064-013-1199-5.
[13] Duncan NW, Wiebking C, Northoff G. Associations of regional GABA and glutamate with intrinsic and extrinsic neural activity in humans – A review of multimodal imaging studies. Neurosci Biobehav Rev 2014;47C:36–52. http://dx.doi.org/10.1016/j.neubiorev.2014.07.016.
[14] Northoff G, Walter M, Schulte RF, et al. GABA concentrations in the human anterior cingulate cortex predict negative BOLD responses in fMRI. Nat Neurosci 2007;10:1515–7. http://dx.doi.org/10.1038/nn2001.
[15] Hu Y, Chen X, Gu H, Yang Y. Resting-state glutamate and GABA concentrations predict task-induced deactivation in the default mode network. J Neurosci 2013;33:18566–73. http://dx.doi.org/10.1523/JNEUROSCI.1973-13.2013.
[16] Kapogiannis D, Reiter DA, Willette AA, Mattson MP. Posteromedial cortex glutamate and GABA predict intrinsic functional connectivity of the default mode network. Neuroimage 2013;64:112–9. http://dx.doi.org/10.1016/j.neuroimage.2012.09.029.
[17] Riese F, Gietl A, Zölch N, et al. Posterior cingulate γ-aminobutyric acid and glutamate/glutamine are reduced in amnestic mild cognitive impairment and are unrelated to amyloid deposition and apolipoprotein E genotype. Neurobiol Aging 2014. http://dx.doi.org/10.1016/j.neurobiolaging.2014.07.030.
[18] Gao JL, Cheung RTF, Chan YS, Chu LW, Lee TMC. Increased prospective memory interference in normal and pathological aging: different roles of motor and verbal processing speed. Neuropsychol Dev Cogn B Aging Neuropsychol Cogn 2013;20:80–100. http://dx.doi.org/10.1080/13825585.2012.672948.
[19] Yizhar O, Fenno LE, Prigge M, et al. Neocortical excitation/inhibition balance in information processing and social dysfunction. Nature 2011;477:171–8. http://dx.doi.org/10.1038/nature10360.
[20] Palop JJ, Mucke L, Roberson ED. Quantifying biomarkers of cognitive dysfunction and neuronal network hyperexcitability in mouse models of Alzheimer's disease: depletion of calcium-dependent proteins and inhibitory hippocampal remodeling. Methods Mol Biol 2011;670:245–62. http://dx.doi.org/10.1007/978-1-60761-744-0_17.
[21] Palop JJ, Mucke L. Amyloid-? induced neuronal dysfunction in Alzheimer's disease: from synapses toward neural networks. Nat Neurosci 2010;13:812–8. http://dx.doi.org/10.1038/nn.2583.
[22] Dayan E, Censor N, Buch ER, Sandrini M, Cohen LG. Noninvasive brain stimulation: from physiology to network dynamics and back. Nat Neurosci 2013;16:838–44. http://dx.doi.org/10.1038/nn.3422.
[23] Huang Y-Z, Edwards MJ, Rounis E, Bhatia KP, Rothwell JC. Theta burst stimulation of the human motor cortex. Neuron 2005;45:201–6. http://dx.doi.org/10.1016/j.neuron.2004.12.033.
[24] Huang Y-Z, Chen R-S, Rothwell JC, Wen H-Y. The after-effect of human theta burst stimulation is NMDA receptor dependent. Clin Neurophysiol 2007;118:1028–32. http://dx.doi.org/10.1016/j.clinph.2007.01.021.
[25] Stagg CJ, Wylezinska M, Matthews PM, et al. Neurochemical effects of theta burst stimulation as assessed by magnetic resonance spectroscopy. J Neurophysiol 2009;101:2872–7. http://dx.doi.org/10.1152/jn.91060.2008.
[26] Vidal-Piñeiro D, Martin-Trias P, Arenaza-Urquijo EM, et al. Task-dependent activity and connectivity predict episodic memory network-based responses to brain stimulation in healthy aging. Brain Stimul 2014. http://dx.doi.org/10.1016/j.brs.2013.12.016.
[27] Ridding MC, Ziemann U. Determinants of the induction of cortical plasticity by non-invasive brain stimulation in healthy subjects. J Physiol 2010;588:2291–304. http://dx.doi.org/10.1113/jphysiol.2010.190314.
[28] Lee TG, D'Esposito M. The dynamic nature of top-down signals originating from prefrontal cortex: a combined fMRI-TMS study. J Neurosci 2012;32:15458–66. http://dx.doi.org/10.1523/JNEUROSCI.0627-12.2012.
[29] Halko MA, Eldaief MC, Horvath JC, Pascual-Leone A. Combining transcranial magnetic stimulation and FMRI to examine the default mode network. J Vis Exp 2010. http://dx.doi.org/10.3791/2271.
[30] Wang JX, Rogers LM, Gross EZ, et al. Targeted enhancement of cortical-hippocampal brain networks and associative memory. Science 2014;345:1054–7. http://dx.doi.org/10.1126/science.1252900.
[31] Eldaief MC, Halko MA, Buckner RL, Pascual-Leone A. Transcranial magnetic stimulation modulates the brain's intrinsic activity in a frequency-dependent manner. Proc Natl Acad Sci U S A 2011;108:21229–34. http://dx.doi.org/10.1073/pnas.1113103109.
[32] Capotosto P, Babiloni C, Romani GL, Corbetta M. Resting-state modulation of alpha rhythms by interference with angular gyrus activity. J Cogn Neurosci 2013. http://dx.doi.org/10.1162/jocn_a_00460.
[33] Clark VP, Coffman BA, Trumbo MC, Gasparovic C. Transcranial direct current stimulation (tDCS) produces localized and specific alterations in neurochemistry: a ^{1}H magnetic resonance spectroscopy study. Neurosci Lett 2011;500:67–71. http://dx.doi.org/10.1016/j.neulet.2011.05.244.
[34] Hunter MA, Coffman BA, Gasparovic C, Calhoun VD, Trumbo MC, Clark VP. Baseline effects of transcranial direct current stimulation on glutamatergic neurotransmission and large-scale network connectivity. Brain Res 2014. http://dx.doi.org/10.1016/j.brainres.2014.09.066.
[35] Marjańska M, Lehéricy S, Valabrègue R, et al. Brain dynamic neurochemical changes in dystonic patients: a magnetic resonance spectroscopy study. Mov Disord 2013;28:201–9. http://dx.doi.org/10.1002/mds.25279.
[36] Stagg CJ, Best JG, Stephenson MC, et al. Polarity-sensitive modulation of cortical neurotransmitters by transcranial stimulation. J Neurosci 2009;29:5202–6. http://dx.doi.org/10.1523/JNEUROSCI.4432-08.2009.
[37] Stagg CJ, Bachtiar V, Johansen-Berg H. The role of GABA in human motor learning. Curr Biol 2011;21:480–4. http://dx.doi.org/10.1016/j.cub.2011.01.069.
[38] Floyer-Lea A, Wylezinska M, Kincses T, Matthews PM. Rapid modulation of GABA concentration in human sensorimotor cortex during motor learning. J Neurophysiol 2006;95:1639–44. http://dx.doi.org/10.1152/jn.00346.2005.
[39] Michels L, Martin E, Klaver P, et al. Frontal GABA levels change during working memory. PLoS One 2012;7:e31933. http://dx.doi.org/10.1371/journal.pone.0031933.
[40] Rossi S, Hallett M, Rossini PM, Pascual-Leone A. Safety, ethical considerations, and application guidelines for the use of transcranial magnetic stimulation in clinical practice and research. Clin Neurophysiol 2009;120:2008–39. http://dx.doi.org/10.1016/j.clinph.2009.08.016.
[41] Rademacher J, Galaburda AM, Kennedy DN, Filipek PA, Caviness VS. Human cerebral cortex: localization, parcellation, and morphometry with magnetic resonance imaging. J Cogn Neurosci 1992;4:352–74. http://dx.doi.org/10.1162/jocn.1992.4.4.352.
[42] Vincent JL, Kahn I, Snyder AZ, Raichle ME, Buckner RL. Evidence for a frontoparietal control system revealed by intrinsic functional connectivity. J Neurophysiol 2008;100:3328–42. http://dx.doi.org/10.1152/jn.90355.2008.
[43] Provencher SW. Estimation of metabolite concentrations from localized in vivo proton NMR spectra. Magn Reson Med 1993;30:672–9.
[44] Govindaraju V, Young K, Maudsley AA. Proton NMR chemical shifts and coupling constants for brain metabolites. NMR Biomed 2000;13:129–53.

[45] Tremblay S, Beaulé V, Proulx S, et al. Relationship between transcranial magnetic stimulation measures of intracortical inhibition and spectroscopy measures of GABA and glutamate + glutamine. J Neurophysiol 2013;109:1343–9. http://dx.doi.org/10.1152/jn.00704.2012.
[46] Ziemann U, Paulus W, Nitsche MA, et al. Consensus: motor cortex plasticity protocols. Brain Stimul 2008;1:164–82. http://dx.doi.org/10.1016/j.brs.2008.06.006.
[47] Bestmann S, Swayne O, Blankenburg F, et al. Dorsal premotor cortex exerts state-dependent causal influences on activity in contralateral primary motor and dorsal premotor cortex. Cereb Cortex 2008;18:1281–91. http://dx.doi.org/10.1093/cercor/bhm159.
[48] Vidal-Piñeiro D, Valls-Pedret C, Fernández-Cabello S, et al. Decreased default mode network connectivity correlates with age-associated structural and cognitive changes. Front Aging Neurosci 2014;6:256. http://dx.doi.org/10.3389/fnagi.2014.00256.
[49] Horn A, Ostwald D, Reisert M, Blankenburg F. The structural-functional connectome and the default mode network of the human brain. Neuroimage 2013. http://dx.doi.org/10.1016/j.neuroimage.2013.09.069.
[50] Rozzi S, Calzavara R, Belmalih A, et al. Cortical connections of the inferior parietal cortical convexity of the macaque monkey. Cereb Cortex 2006;16:1389–417. http://dx.doi.org/10.1093/cercor/bhj076.
[51] Caspers S, Eickhoff SB, Rick T, et al. Probabilistic fibre tract analysis of cytoarchitectonically defined human inferior parietal lobule areas reveals similarities to macaques. Neuroimage 2011;58:362–80. http://dx.doi.org/10.1016/j.neuroimage.2011.06.027.
[52] Morecraft RJ, Cipolloni PB, Stilwell-Morecraft KS, Gedney MT, Pandya DN. Cytoarchitecture and cortical connections of the posterior cingulate and adjacent somatosensory fields in the rhesus monkey. J Comp Neurol 2004;469:37–69. http://dx.doi.org/10.1002/cne.10980.
[53] Pandya DN, Seltzer B. Intrinsic connections and architectonics of posterior parietal cortex in the rhesus monkey. J Comp Neurol 1982;204:196–210. http://dx.doi.org/10.1002/cne.902040208.
[54] Khalsa S, Mayhew SD, Chechlacz M, Bagary M, Bagshaw AP. The structural and functional connectivity of the posterior cingulate cortex: comparison between deterministic and probabilistic tractography for the investigation of structure-function relationships. Neuroimage 2013. http://dx.doi.org/10.1016/j.neuroimage.2013.12.022.
[55] Hagmann P, Cammoun L, Gigandet X, et al. Mapping the structural core of human cerebral cortex. PLoS Biol 2008;6:e159. http://dx.doi.org/10.1371/journal.pbio.0060159.
[56] Greicius MD, Supekar K, Menon V, Dougherty RF. Resting-state functional connectivity reflects structural connectivity in the default mode network. Cereb Cortex 2009;19:72–8. http://dx.doi.org/10.1093/cercor/bhn059.
[57] Deng Z-D, Lisanby SH, Peterchev AV. Electric field depth-focality tradeoff in transcranial magnetic stimulation: simulation comparison of 50 coil designs. Brain Stimul 2013;6:1–13. http://dx.doi.org/10.1016/j.brs.2012.02.005.
[58] Heise K-F, Zimerman M, Hoppe J, Gerloff C, Wegscheider K, Hummel FC. The aging motor system as a model for plastic changes of GABA-mediated intracortical inhibition and their behavioral relevance. J Neurosci 2013;33:9039–49. http://dx.doi.org/10.1523/JNEUROSCI.4094-12.2013.
[59] Burke SN, Barnes CA. Neural plasticity in the ageing brain. Nat Rev Neurosci 2006;7:30–40. http://dx.doi.org/10.1038/nrn1809.
[60] Oberman L, Eldaief M, Fecteau S, Ifert-Miller F, Tormos JM, Pascual-Leone A. Abnormal modulation of corticospinal excitability in adults with Asperger's syndrome. Eur J Neurosci 2012;36:2782–8. http://dx.doi.org/10.1111/j.1460-9568.2012.08172.x.
[61] Battaglia F, Wang H-Y, Ghilardi MF, et al. Cortical plasticity in Alzheimer's disease in humans and rodents. Biol Psychiatry 2007;62:1405–12. http://dx.doi.org/10.1016/j.biopsych.2007.02.027.
[62] Buckner RL, Snyder AZ, Shannon BJ, et al. Molecular, structural, and functional characterization of Alzheimer's disease: evidence for a relationship between default activity, amyloid, and memory. J Neurosci 2005;25:7709–17. http://dx.doi.org/10.1523/JNEUROSCI.2177-05.2005.
[63] Friedman SD, Baker LD, Borson S, et al. Growth hormone-releasing hormone effects on brain γ-aminobutyric acid levels in mild cognitive impairment and healthy aging. JAMA Neurol 2013;70:883–90. http://dx.doi.org/10.1001/jamaneurol.2013.1425.
[64] Gusnard DA, Raichle ME, Raichle ME. Searching for a baseline: functional imaging and the resting human brain. Nat Rev Neurosci 2001;2:685–94. http://dx.doi.org/10.1038/35094500.
[65] Deco G, Jirsa V, McIntosh AR, Sporns O, Kötter R. Key role of coupling, delay, and noise in resting brain fluctuations. Proc Natl Acad Sci U S A 2009;106:10302–7. http://dx.doi.org/10.1073/pnas.0901831106.
[66] Dastjerdi M, Foster BL, Nasrullah S, et al. Differential electrophysiological response during rest, self-referential, and non-self-referential tasks in human posteromedial cortex. Proc Natl Acad Sci U S A 2011;108:3023–8. http://dx.doi.org/10.1073/pnas.1017098108.
[67] Hayden BY, Smith DV, Platt ML. Electrophysiological correlates of default-mode processing in macaque posterior cingulate cortex. Proc Natl Acad Sci U S A 2009;106:5948–53. http://dx.doi.org/10.1073/pnas.0812035106.
[68] Todd G, Ridding MC. The response to repetitive stimulation of human motor cortex is influenced by the history of synaptic activity. Restor Neurol Neurosci 2010;28:459–67. http://dx.doi.org/10.3233/RNN-2010-0565.
[69] Palomero-Gallagher N, Vogt BA, Schleicher A, Mayberg HS, Zilles K. Receptor architecture of human cingulate cortex: evaluation of the four-region neurobiological model. Hum Brain Mapp 2009;30:2336–55. http://dx.doi.org/10.1002/hbm.20667.
[70] Economo CF von, Koskinas GN. Atlas of cytoarchitectonics of the adult human cerebral cortex. S Karger AG; 2008.
[71] Guggisberg AG, Dubach P, Hess CW, Wüthrich C, Mathis J. Motor evoked potentials from masseter muscle induced by transcranial magnetic stimulation of the pyramidal tract: the importance of coil orientation. Clin Neurophysiol 2001;112:2312–9.
[72] Nitsche MA, Müller-Dahlhaus F, Paulus W, Ziemann U. The pharmacology of neuroplasticity induced by non-invasive brain stimulation: building models for the clinical use of CNS active drugs. J Physiol 2012;590:4641–62. http://dx.doi.org/10.1113/jphysiol.2012.232975.
[73] Falkenberg LE, Westerhausen R, Specht K, Hugdahl K. Resting-state glutamate level in the anterior cingulate predicts blood-oxygen level-dependent response to cognitive control. Proc Natl Acad Sci U S A 2012;109:5069–73. http://dx.doi.org/10.1073/pnas.1115628109.
[74] Strafella AP, Paus T, Barrett J, Dagher A. Repetitive transcranial magnetic stimulation of the human prefrontal cortex induces dopamine release in the caudate nucleus. J Neurosci 2001;21:RC157.
[75] Strafella AP, Paus T, Fraraccio M, Dagher A. Striatal dopamine release induced by repetitive transcranial magnetic stimulation of the human motor cortex. Brain J Neurol 2003;126:2609–15. http://dx.doi.org/10.1093/brain/awg268.
[76] Cho SS, Strafella AP. rTMS of the left dorsolateral prefrontal cortex modulates dopamine release in the ipsilateral anterior cingulate cortex and orbitofrontal cortex. PLoS One 2009;4:e6725. http://dx.doi.org/10.1371/journal.pone.0006725.
[77] Fox MD, Buckner RL, White MP, Greicius MD, Pascual-Leone A. Efficacy of transcranial magnetic stimulation targets for depression is related to intrinsic functional connectivity with the subgenual cingulate. Biol Psychiatry 2012;72:595–603. http://dx.doi.org/10.1016/j.biopsych.2012.04.028.
[78] Fox MD, Snyder AZ, Vincent JL, Corbetta M, Van Essen DC, Raichle ME. The human brain is intrinsically organized into dynamic, anticorrelated functional networks. Proc Natl Acad Sci U S A 2005;102:9673–8. http://dx.doi.org/10.1073/pnas.0504136102.
[79] Stagg CJ. Magnetic resonance spectroscopy as a tool to study the role of GABA in motor-cortical plasticity. Neuroimage 2014;86:19–27. http://dx.doi.org/10.1016/j.neuroimage.2013.01.009.
[80] Mars RB, Jbabdi S, Sallet J, et al. Diffusion-weighted imaging tractography-based parcellation of the human parietal cortex and comparison with human and macaque resting-state functional connectivity. J Neurosci 2011;31:4087–100. http://dx.doi.org/10.1523/JNEUROSCI.5102-10.2011.
[81] Uddin LQ, Supekar K, Amin H, et al. Dissociable connectivity within human angular gyrus and intraparietal sulcus: evidence from functional and structural connectivity. Cereb Cortex 2010;20:2636–46. http://dx.doi.org/10.1093/cercor/bhq011.
[82] Stagg CJ, Bestmann S, Constantinescu AO, et al. Relationship between physiological measures of excitability and levels of glutamate and GABA in the human motor cortex. J Physiol 2011;589:5845–55. http://dx.doi.org/10.1113/jphysiol.2011.216978.
[83] Mullins PG, McGonigle DJ, O'Gorman RL, et al. Current practice in the use of MEGA-PRESS spectroscopy for the detection of GABA. Neuroimage 2014;86:43–52. http://dx.doi.org/10.1016/j.neuroimage.2012.12.004.